Imprinted labyrinths and percolation in Nd-Co/Nb magnetic/superconducting hybrids

L. Ruiz-Valdepeñas, M. Velez, F. Valdés-Bango, L. M. Alvarez-Prado, F. J. Garcia-Alonso, J. I. Martin, E. Navarro, J. M. Alameda, and J. L. Vicent

---

Articles you may be interested in

Nature of magnetic domains in an exchange coupled BiFeO3/CoFe heterostructure
Appl. Phys. Lett. 102, 112902 (2013); 10.1063/1.4795794

Magnetization reversal and microstructure of [(Nd 2 Fe 14 B) x∕Nb] n films
J. Appl. Phys. 99, 053901 (2006); 10.1063/1.2174114

Reversible magnetization processes and energy density product in Sm–CoFe and Sm–Co/Co bilayers
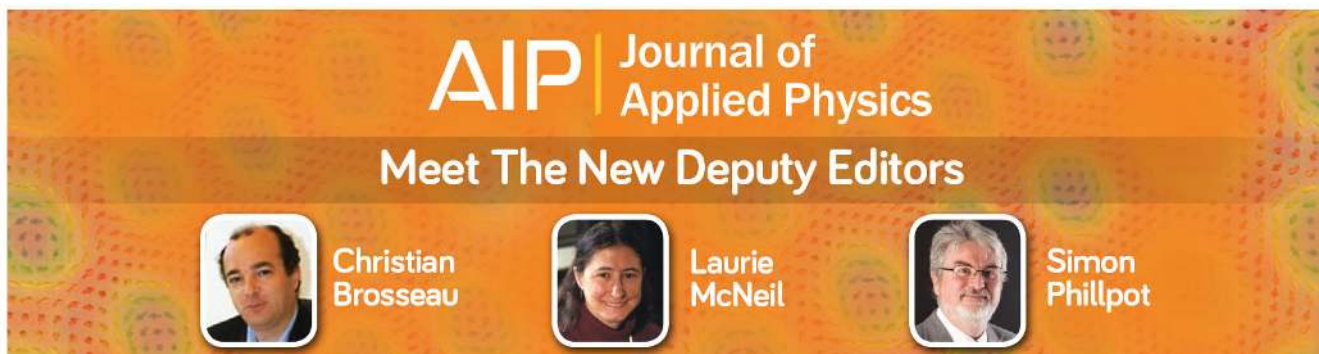J. Appl. Phys. 93, 6489 (2003); 10.1063/1.1558245

Remagnetization processes in SmCo/NdCo exchange springs
J. Appl. Phys. 93, 6486 (2003); 10.1063/1.1541634

Exchange coupling in epitaxial Sm–Co (1100)/ Nd–Co exchange-spring bilayers
J. Appl. Phys. 93, 8122 (2003); 10.1063/1.1538180

Imprinted labyrinths and percolation in Nd-Co/Nb magnetic/superconducting hybrids

L. Ruiz-Valdepeñas,[1] M. Velez,[2,3] F. Valdés-Bango,[2,3] L. M. Alvarez-Prado,[2,3]
F. J. Garcia-Alonso,[3,4] J. I. Martin,[2,3] E. Navarro,[1] J. M. Alameda,[2,3] and J. L. Vicent[1,5]

[1]Dpto. Física de Materiales, Universidad Complutense, 28040 Madrid, Spain
[2]Dpto. Física, Universidad de Oviedo, 33007 Oviedo, Spain
[3]CINN (CSIC-Universidad de Oviedo), Llanera, Spain
[4]Depto. Química Orgánica e Inorgánica, Universidad de Oviedo, 33007 Oviedo, Spain
[5]IMDEA-Nanociencia, Cantoblanco, 28049 Madrid, Spain

Magnetization reversal processes have been studied in hybrid magnetic/superconducting Nd-Co/Nb bilayers by the comparison of out-of-plane magnetic hysteresis loops and superconducting phase diagrams as a function of magnetic layer thickness and of disorder in the magnetic layer induced by a nanostructured copolymer template. A good correlation is found between the regimes corresponding to percolation effects in the superconductor and to the transition from extended to confined superconductivity with the characteristic fields for reverse domain nucleation and fast domain expansion in the magnetic layer, indicating that superconductivity nucleates on the disordered network imprinted on the superconducting layer by the labyrinth domain structure of the magnetic layer. As disorder increases in the magnetic layer, percolation effects disappear from the superconducting transitions in agreement with a more homogeneous magnetization reversal process. © 2014 AIP Publishing LLC. [http://dx.doi.org/10.1063/1.4881277]

I. INTRODUCTION

Magnetic domain structures in perpendicular magnetic anisotropy (PMA) thin films have been intensively studied due to their potential in magnetic recording applications.[1] Depending on magnetic history and material parameters, a variety of configurations can be observed during the magnetization reversal process ranging from ordered arrays of parallel stripe domains to disordered labyrinthine structures.[2] Different experimental techniques such as magnetic force microscopy (MFM)[3] or X-ray microscopy[4] and theoretical models[5] have shown how the interplay between magnetic anisotropy, dipolar interactions, and disorder affects critically the physics of reverse domain nucleation and expansion and the resulting domain structure.

Magnetic domains in PMA materials have also been used to modify the superconducting properties of hybrid magnetic/superconducting (FM/SC) multilayers and nanostructures.[6] A rich variety of behaviors has been described in FM/SC hybrids,[7] such as reentrant superconductivity,[6] domain wall induced superconductivity,[8] or periodic pinning[9] due to the interplay between these two long range order phenomena. In general, a ferromagnetic layer in close proximity to a superconductor modifies its superconducting properties both through the exchange interaction and through the effect of the localized stray field.[7] Thus, the strong and localized stray fields created by domains in PMA films provide an interesting tool to control superconductivity nucleation:[6,10,11] for example, ordered stripe domain patterns could be used to create anisotropic and tunable pinning potentials for the vortex lattice.[12] On the other hand, this sensitivity of the superconducting properties to ferromagnetic domains could be used to obtain information on domain configuration within the ferromagnetic layer. Very recently, it has been shown

how the labyrinthine domain patterns in a perpendicular magnetic anisotropy Nd-Co film can be used to imprint a fractal superconducting wire network in a neighboring Nb layer[13] with dimensionality and percolation properties given by the connectivity of the underlying magnetic domain structure.

In this work, we have studied the superconducting properties of hybrid magnetic/superconducting Nd-Co/Nb bilayers along the first stages of the magnetization reversal process of the magnetic layer, which correspond to the regime dominated by percolation effects in the superconductor. Two strategies have been used to modify domain configuration in the amorphous Nd-Co layer: first, magnetic layer thickness has been varied in order to tune the interplay between dipolar and anisotropy energies; and second, a series of Nd-Co layers has been prepared on Si substrates covered by a nanostructured diblock copolymer template[14] in order to enhance disorder in the magnetic layer. Changes in the superconducting properties of the hybrid system have been correlated to differences in magnetization reversal of the magnetic layer.

II. EXPERIMENTAL

Two series of ferromagnetic/superconducting Nd-Co/Nb bilayers have been grown by sputtering changing magnetic layer thickness t and type of substrate. The first series of Nd-Co/Nb bilayers is grown on Si (100) substrates with variable magnetic layer thickness in the 30 nm–80 nm range. Sample deposition takes place in a two step process:[13] first, a (10 nm Al/amorphous $NdCo_5$/5 nm Al) trilayer is grown on the chosen substrate by cosputtering; and then, it is taken out of the chamber so that the 5 nm thick Al capping layer becomes oxidized. Finally, a 50 nm thick Nb layer is grown on top of the trilayer in order to obtain the hybrid ferromagnetic/superconducting structure, as sketched in Fig. 1(a). The purpose
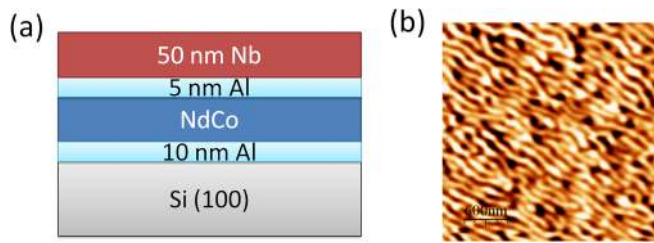
FIG. 1. (a) Sketch of Ferromagnetic/Superconducting Nd-Co/Nb multilayer. (b) MFM image of stripe domains in a 60 nm thick Nd-Co film measured at remanence after in plane saturation with H = 1 kOe at room temperature.

of the oxidized AlO_x interlayer is to minimize exchange induced proximity effects, so that the observed changes in the superconducting properties of the hybrid system can be attributed to the role of stray fields created on the Nb layers by the domain structure in the Nd-Co layers.

A second series of Nd-Co/Nb bilayers has been prepared in a similar fashion but on Si substrates covered by a di-block copolymer template (preparation details can be found in Ref. 14). These nanostructured templates modify both the magnetic film topography and mechanical strain on a local scale, resulting in a reduction in PMA anisotropy and an enhancement of stripe domain pinning effects, which could be of use to alter the geometry of the imprinted superconducting network in the Nb layer.

In the following, we will refer to these two series of samples as Si/Nd-Co(t)/Nb and copolymer/Nd-Co(t)/Nb, respectively, where t indicates magnetic layer thickness in nm.

The superconducting properties of the Nb layer in the hybrid system have been characterized on control 50 nm thick Nb layers grown on bare Si substrates. Superconducting transition temperature is $T_C \approx 7.55$ K and Ginzburg-Landau coherence length, estimated from the temperature dependence of the upper critical field $H_{c2}(T)$, is $\xi_{GL} = 9$ nm, typical of sputtering-grown Nb films in this thickness range.[15]

The ferromagnetic layer in the hybrid bilayers is made of $NdCo_5$, an amorphous alloy with saturation magnetization $M_S = 1.4 \times 10^3$ emu/cm^3 at 10 K.[16] Out of plane hysteresis loops present typical saturation fields $H_{sat}^{out-of-plane}$ in the 5–10 kOe range, depending on sample thickness, well below the shape anisotropy field $4\pi M_S = 18$ kOe indicating the existence of a moderate out-of-plane anisotropy K_n within the layers.[16] The effective PMA constant, K_n, can be estimated from $H_{sat}^{in-plane} = 25$ kOe, the saturation field of an in-plane hysteresis loop measured in a 80 nm thick film,[16] as $K_n = \frac{1}{2} H_{sat}^{in-plane} M_S = 1.8 \times 10^7$ erg/cm^3. Thus, we may estimate the

anisotropy ratio as $Q = K_n/2\pi M_s^2 \approx 1.4$. A detailed structural characterization of these amorphous Nd-Co films by EXAFS and X-ray Magnetic Circular Dichroism[17] suggests that the origin of PMA is mainly related to the atomic environment to first neighbors of the Nd atoms.

Different metastable domain structures can be found at remanence in this kind of amorphous rare earth-transition metal films:[13,18] from parallel stripe domains with alternating sign of the out-of-plane magnetization component as shown in the MFM image of Fig. 1(b) after applying a large in-plane magnetic field to disordered labyrinthine configurations, which are often observed after applying out-of-plane magnetic fields. Due to the interplay between PMA and dipolar energy, the characteristic parameters of the stripe domain configuration such as stripe domain period Λ and out-of-plane magnetization component are strongly dependent on magnetic film thickness. For this reason, micromagnetic simulations have been used to study the effects of changing the magnetic layer thickness on the stripe domain structure of the Nd-Co layer[19] and, also, to calculate the stray field created on the Nb layer. Simulations have been performed at remanence in an ordered parallel stripe geometry, adjusting material parameters to fit the results of MFM characterization and macroscopic hysteresis loops.[13]

The superconducting and magnetic properties of the Nd-Co/Nb bilayers have been characterized by magnetotransport in a He cryostat with a 90 kOe superconducting solenoid using a four probe DC technique,[20] with an applied current I = 10-100 μA. First, out-of-plane hysteresis loops of the Nd-Co layers have been measured by Extraordinary Hall Effect (EHE), making use of the much larger Hall effect in ferromagnetic materials such as Nd-Co than in ordinary metals such as Nb.[21] EHE loops have been obtained at 10 K, i.e., just above the superconducting transition. Second, the superconductive resistive transitions R(T) have been acquired under a constant out-of-plane magnetic field H. This field has been sequentially varied in order to follow the changes in the superconducting behavior of the samples along the ascending and descending branches of the hysteresis loop in the magnetic layer.

III. RESULTS AND DISCUSSION

A. Domain structure in Nd-Co layers

Figure 2 shows the basic parameters of stripe domain configuration, extracted from micromagnetic simulations, as

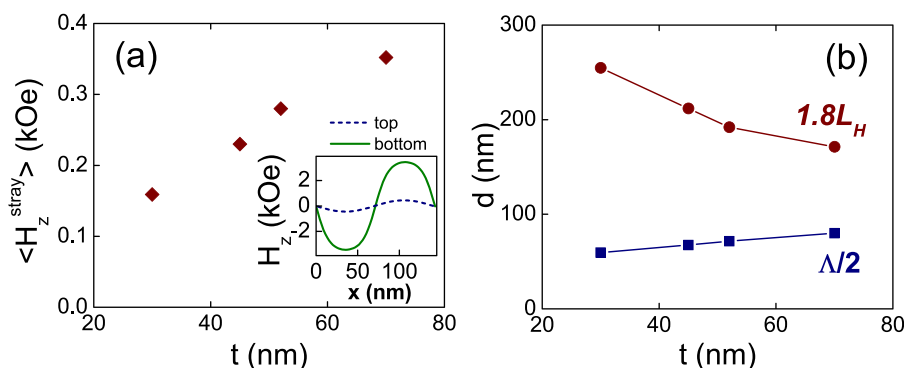FIG. 2. (a) Average stray field created at the top surface of the Nb layer by each stripe domain as a function of Nd-Co layer thickness. Inset shows stray field profile $H_z^{stray}(x)$ created by a 52 nm thick Nd-Co layer at the top and bottom sides of the Nb layer. (b) Stripe domain size $\Lambda/2$ in comparison with the criterium for reentrant superconductivity $1.8L_H$ as a function of magnetic layer thickness.

a function of Nd-Co thickness: average perpendicular stray field $\langle H_z^{stray} \rangle$ in Fig. 2(a) and stripe domain period Λ in Fig. 2(b). Stray fields are, in general, very sensitive to the distance from the magnetic layer. This can be seen, for example, in the stray field profiles $H_z^{stray}(x)$ plotted in the inset of Fig. 2(a) for a 52 nm thick Nd-Co layer, calculated at a distance $z = 5$ nm and $z = 55$ nm over the magnetic layer, respectively (i.e., at the bottom and top surfaces of the Nb film). $H_z^{stray}(x)$ curves present a periodic oscillation within the film plane with period $\Lambda = 143$ nm, following the periodic variations in out-of-plane magnetization component of the underlying parallel stripe domain pattern, with a steeply decreasing amplitude from $H_z^{stray}(max) = 3.5$ kOe at the bottom of the Nb film ($z = 5$ nm) to $H_z^{stray}(max) = 0.44$ kOe at the top side ($z = 55$ nm). In the present case of hybrid superconducting/magnetic systems, nucleation of superconductivity is favored at the film surface with maximum superconducting order parameter,[10] which is the furthest from the magnetic layer. Thus, $\langle H_z^{stray} \rangle$, the spatial average of $H_z^{stray}(x)$ over a positive domain region calculated at the top surface of the Nb layer, has been found to be a good parameter to quantify the strength of interaction in the analysis of superconducting phase diagrams.[13] As shown in Fig. 2(a), $\langle H_z^{stray} \rangle$ increases monotonously from 0.15 to 0.35 kOe as magnetic layer thickness is varied from 30 nm to 70 nm. This dependence can be attributed to an increase in the amplitude of the oscillating out of plane magnetization component in the thicker magnetic films, as indicated by micromagnetic simulations.

From the point of view of the superconducting layer, an $\langle H_z^{stray} \rangle$ enhancement is translated into a smaller size of superconducting nuclei, with a characteristic width given by the magnetic length $L_H = (\Phi_0/2\pi \langle H_z^{stray} \rangle)^{1/2}$.[10] In hybrid SC/FM bilayers, the comparison between L_H and the size of each stripe domain $\Lambda/2$ determines the overlapping between the superconducting nuclei above each magnetic domain and the presence or not of reentrant superconductivity phase diagrams.[22] In particular, for sinusoidal stray field variations, similar to the $H_z^{stray}(x)$ profiles in the inset of Fig. 2(a), magnetic domains can be considered within the small size regime, with no reentrant effects in the hybrid FM/SC system, as long as $\Lambda/2 < 1.8 L_H$.[22] This condition is fulfilled in the whole studied thickness range of the Nd-Co/Nb bilayers, as shown in Fig. 2(b), indicating that all the samples in this work can be considered within the small domain size regime.

B. Superconducting phase boundary in Si/Nd-Co/Nb bilayers

Figure 3 shows the results of the magnetic and superconducting characterization of Si/Nd-Co(75)/Nb and Si/Nd-Co(30)/Nb. In both cases, out-of-plane EHE loops display the typical shape of magnetization reversal through nucleation and fast expansion of reversed domains:[4,23] as the field is decreased from saturation, the magnetization stays virtually constant until, at a positive nucleation field, there is a sharp magnetization jump in a narrow field interval that can be associated to the "avalanche" like expansion of clusters of labyrinthine domains. This jump ends when reversed
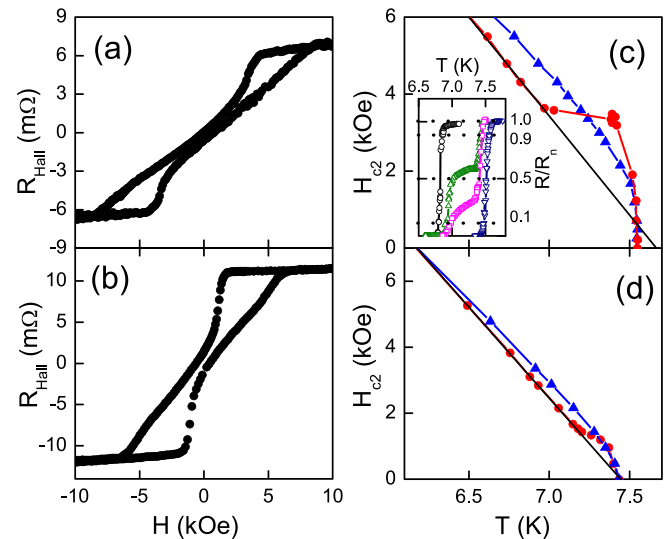

FIG. 3. Extraordinary Hall Effect out-of plane hysteresis loop of Si/Nd-Co(t)/Nb bilayers at 10 K: (a) Si/Nd-Co(75)/Nb and (b) Si/Nd-Co(30)/Nb. Superconducting phase diagrams $H_{c2}^{0.5Rn}(T)$ for: (c) Si/Nd-Co(75)/Nb and (d) Si/Nd-Co(30)/Nbi: ●, curve measured as the field is reduced from out-of-plane saturation at 20 kOe; △, curve obtained upon increasing the field from a disordered remanent state. Straight line indicates the linear temperature dependence characteristic of a plain Nb film. Inset in (c) shows several normalized $R(T)/R_n$ curves of Si/Nd-Co(75)/Nb measured in sequential order along the descending branch of the hysteresis loop: $H = 4.3$ kOe (○), 3.6 kOe (△), 3.4 kOe (□), and 1.9 kOe (◌).

domains fill the sample, already at a positive magnetization value. Then, reversal proceeds following an almost linear magnetization-field dependence in a broad field range around remanence, mostly by reversible domain wall motion. Finally, magnetization reversal is completed at negative. fields by a domain annihilation process, marked by a steeper section in the hysteresis loop The main difference in the magnetic behavior of Si/Nd-Co(75)/Nb (Fig. 3(a)) and Si/Nd- Co(30)/Nb (Fig. 3(b)) is the smaller field scale for the thinner sample which, for constant anisotropy and disorder, can be attributed to the smaller weight of dipolar energy as thickness is reduced.[24]

One of the most interesting features in out-of-plane hysteresis loops of PMA materials is the magnetization jump at the onset of magnetization reversal. It is very sharp in reversal processes characterized by fast expansion of clusters of reversed domains from a few initial reversed nuclei;[23] but in real samples, it becomes rounded due to domain wall pinning effects.[4,25] Actually, as the strength of disorder increases, the system switches over to a nucleation dominated regime with a more homogenous domain structure and the magnetization jump is washed away.[25] However, the transition between expansion dominated and nucleation dominated magnetization reversal processes is relatively gradual so that it is not easy to determine just from the shape of hysteresis loops or, even, from the final geometry of labyrinth domains at remanence.[24] In the case of FM/SC hybrids, the inhomogeneous stray field above reverse magnetic domains can promote the nucleation of superconductivity.[6] Thus, the evolution of the superconducting properties of the SC layer along a hysteresis loop in the FM layer can provide interesting information on the evolution of reverse domain geometry. This can be seen,

for example, in the series of R(T) curves measured in Si/Nd-Co(75)/Nb along the descending branch of the hysteresis loop shown in the inset of Fig. 3(c): at large magnetic fields, superconducting transitions are sharp; then, within a narrow field interval, R(T) curves develop a two step structure characteristic of percolation effects between normal and superconducting regions within the sample; finally, at lower fields, sharp single step R(T) transitions are observed again. Percolation effects in the SC layer imply a heterogeneous superconducting/normal sample structure with large sample areas free of superconducting nuclei (and, therefore, of reversed magnetic domains).[26] This is in agreement with the sharp magnetization jumps observed in these Si/Nd-Co/Nb bilayers, which are characteristic of magnetization reversal through the expansion of clusters of reverse domains which implies a strong fluctuation in the density of reversed domains across the sample.

Superconducting R(T) transitions can be used to obtain the temperature dependent upper critical $H_{c2}(T)$, as the points in the H-T plane in which $R(T,H)$ becomes a certain fraction of the normal state resistance R_n.[6,11,13] Figures 3(c) and 3(d) show the superconducting phase boundaries $H_{c2}(T)$, measured at the midpoint of the superconducting transition ($R(T,H) = 0.5R_n$), along the descending (circles) and ascending (triangles) branches of the hysteresis loop, for Si/Nd-Co(75)/Nb and Si/Nd-Co(30)/Nb, respectively. Both hybrid samples display a qualitatively similar behavior: in the descending branch of the loop, as the field is decreased from out of plane saturation, $H_{c2}(T)$ follows first the typical linear temperature dependence expected for an extended superconducting film in a perpendicular field; then, in a narrow field interval, $H_{c2}(T)$ switches over to a stronger non-linear temperature dependence characteristic of confined superconductivity,[13] i.e., to the superconducting network nucleated on top of the labyrinthine reversed domain structure; on the other hand, in the ascending branch of the loop, the non-linear $H_{c2}(T)$ behavior extends in a much broader

field range. Once again, the main difference between Si/Nd-Co(75)/Nb and Si/Nd-Co(30)/Nb appears in the smaller magnetic field scale in the thinner sample, similar to the results of the magnetic characterization.

The comparison between the relevant field ranges in the EHE loop of the magnetic Nd-Co layer and in the superconducting phase boundary $H_{c2}(T)$ of the superconducting Nb layer can be seen in more detail in Fig. 4(a). First, the characteristic field values of the magnetic loop have been defined as indicated in Fig. 4(b): H_N^{FM}, the nucleation field for reversed domains, has been defined as the first departure from the linear high field R_{Hall} baseline, associated to ordinary Hall effect; and, ΔH^{FM}, the field interval for fast reverse domain expansion, has been defined by the range of steepest magnetization change. Second, the characteristic fields H_1^{SC} and H_2^{SC} for the transition from extended to confined superconductivity have been defined as indicated in Fig. 4(c). For each sample, the superconducting phase boundary measured along the descending branch of the hysteresis loop has been plotted on a reduced temperature scale using two different resistance criteria:

$H_{c2}^{0.9Rn}(T)$ calculated from $R(T,H) = 0.9R_n$ and $H_{c2}^{0.1Rn}(T)$ calculated from $R(T,H) = 0.1R_n$. At high and low fields, both curves are superimposed on each other, as corresponds to a homogeneous sample behavior with narrow superconducting transitions. However, in the intermediate field range dominated by percolation effects, these two curves differ significantly due to the presence of steps in the R(T) transitions. The high field behavior has been fitted to $H_{c2} \sim (1-T/T_C)$, typical of an extended superconducting film (dashed line in Fig. 4(c)), whereas the low field behavior has been fitted to $H_{c2} \sim (1-T/T_C)^{0.66}$, characteristic of confined superconductivity on the fractal network imprinted by the labyrinthine domain structure[13] (solid line in Fig. 4(c)). Then, H_1^{SC} has been defined as the field in which $H_{c2}^{0.9Rn}(T)$ departs from linearity, indicating the presence of the first confined superconductivity regions within the
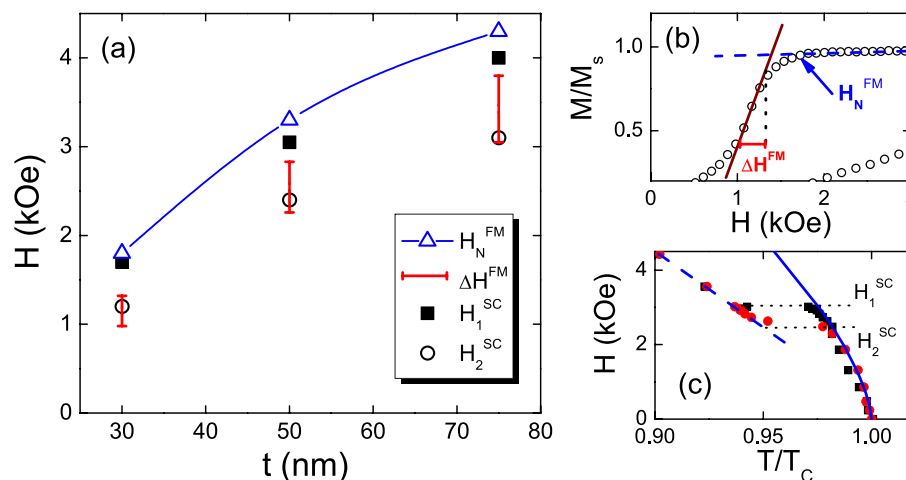

FIG. 4. (a) Thickness dependence of the different characteristic fields in Si/Nd-Co(t)/Nb bilayers: H_N^{FM}, nucleation field of reversed domains in EHE loop; ΔH^{FM}, field interval of maximum slope in EHE loop; H_1^{SC}-H_2^{SC}, field interval for the transition from linear $H_{c2}(T)$ (extended superconducting film) to non-linear $H_{c2}(T)$ (confined superconductivity). (b) Detail of EHE loop of Si/Nd-Co(30)/Nb showing the definition of ΔH^{FM} from the region of maximum slope; (c) Detail of superconducting phase diagrams of Si/Nd-Co(52)/Nb showing the definition of ΔH_{sup}: ■, $H_{c2}^{0.9Rn}(T)$; ○, $H_{c2}^{0.1Rn}(T)$. Dashed line is a fit to a linear $H_{c2}(T)$. Solid line is a fit to $H_{c2}(T) \sim (1-T/T_C)^{0.66}$ characteristic of confined superconductivity. Temperature axis has been normalized by the zero field transition temperature in each case.

TABLE I. Comparison of the characteristic parameters of reverse domain expansion and percolation processes in Si/Nd-Co/Nb and copolymer/Nd-Co/Nb bilayers.

t (nm)	Si/Nd-Co(t)/Nb			Copolymer/Nd-Co(t)/Nb		
	H_N^{FM} (kOe)	ΔH^{FM}(kOe)	p_c	H_N^{FM} (kOe)	ΔH^{FM}(kOe)	p_c
30	1.8	0.3	0.18	3.0	no jump	…
52	3.3	0.6	0.19	3.8	1.7	0.30
75	4.3	0.8	0.17	4.5	0.8	0.19

sample. Finally, H_2^{SC} has been defined as the field in which $H_{c2}^{0.1Rn}$(T) adopts the non-linear temperature dependence indicating the disappearance of the last extended superconducting regions from the sample.

The correlation between magnetic and superconducting data is very clear: first, H_N^{FM} and H_1^{SC} present very similar values in all the FM/SC bilayers indicating that both of them are associated with the same phenomenon but measured with a different technique: confined superconducting regions appear in the Nb film reducing the total resistance as soon as the first magnetic reversed domains are nucleated in the Nd-Co layer. Second, H_2^{SC} is located within ΔH^{FM} indicating that full percolation of the superconducting network nucleated on top of the labyrinthine reverse magnetic domains always happens during the stage of fast reverse domain expansion.

The fraction of reversed domains at percolation can be estimated from M_2^{SC}, the magnetization value at H_2^{SC}, as $p_c = 0.5(1 - M_2^{SC}/M_s)$ (see Table I). It presents very similar values in all the Si/Nd-Co/Nb samples, indicating that the basic topology of the percolating cluster is the same independently of FM layer thickness. The percolation threshold lies in the range $p_c = 0.17$–0.19, well below the theoretical percolation threshold for square lattice models $p_c = 0.5$. These low thresholds are typical of double percolation,[27] which, in these FM/SC hybrids,[13] can be associated to the different length scales of reverse domain nucleation and expansion phenomena.

C. Superconducting phase boundary in copolymer/Nd-Co/Nb bilayers

The role of increasing disorder in magnetization reversal and percolation processes in these PMA Nd-Co/Nb bilayers

has been studied in a series of copolymer/Nd-Co/Nb bilayers. A comparison between the relevant field parameters of the out-of-plane EHE hysteresis loops of Si/Nd-Co/Nb and copolymer/Nd-Co/Nb samples can be found in Table I. For the same magnetic sample thickness, the onset of magnetization reversal occurs at similar H_N^{FM} values that decrease monotonously as t is reduced, due to the reduction in the dipolar energy term. The main differences between both series of samples appear in the steepness of the initial magnetization jump: for $t = 75$ nm, the same $\Delta H^{FM} = 0.8$ kOe is found in both cases. For $t = 52$ nm, an opposite trend is observed with a decrease down to $\Delta H^{FM} = 0.6$ kOe for Si/Nd-Co(52)/Nb and an increase up to $\Delta H^{FM} = 1.7$ kOe for copolymer/Nd-Co(52)/Nb. Finally, for $t = 30$ nm, ΔH^{FM} is reduced again down to 0.3 kOe for Si/Nd-Co(30)/Nb, following the decrease in H_N^{FM} whereas no magnetization jump can be defined in the EHE loop of copolymer/Nd-Co(30)/Nb, suggesting the transition to a nucleation dominated magnetization reversal process due to the enhanced disorder.

The analysis of the percolation process in the superconducting transitions of copolymer/Nd-Co/Nb bilayers provides further support to this idea. Figure 5 shows several superconducting R(T) curves measured in the descending field branch of the out-of-plane hysteresis loop, just below the nucleation field for reverse magnetic domains H_N^{FM}. A clear two step transition, similar to the behavior of the Si/Nd-Co/Nb series, is only observed for copolymer/Nd-Co(75)/Nb (see Fig. 5(a)). Then, as the thickness of magnetic layer decreases, this two step structure becomes rounded for copolymer/Nd-Co(52)/Nb. Finally, percolation effects disappear for copolymer/Nd-Co(30)/Nb and the superconducting transitions present a similar 0.1 K width along the whole field range corresponding to magnetization reversal in the Nd-Co layer. This indicates a more homogeneous nucleation of superconductivity in the sample with the thinnest magnetic layer, as corresponds to a homogenous distribution of reversed magnetic domains in a nucleation dominated magnetization reversal process.

These changes in the shapes of R(T) curves also appear in the superconducting phase diagrams H_{c2}(T) shown in Fig. 6, for Si/Nd-Co(52)/Nb and copolymer/Nd-Co(52)/Nb. The main consequence of changing the substrate from plain Si to copolymer template is noticed as a smoothing of the
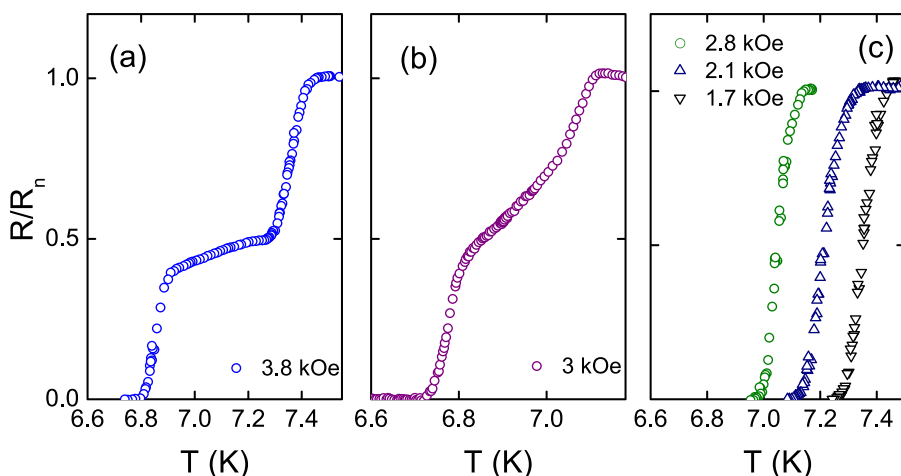

FIG. 5. Typical superconducting R(T)/R_n transitions measured in the descending branch of the hysteresis loop under a constant H, just below H_N^{FM}: (a) copolymer/Nd-Co(75)/Nb; (b) copolymer/Nd-Co(52)/Nb; and (c) copolymer/Nd-Co(30)/Nb.
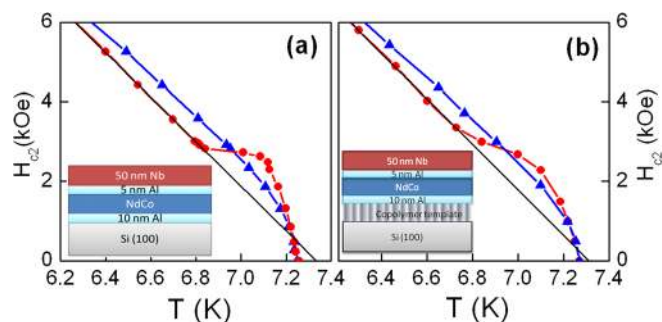
FIG. 6. Superconducting phase diagrams $H_{c2}^{0.5}R_n(T)$ for: (a) Si/Nd-Co(52)/Nb; (b) copolymer/Nd-Co(52)/Nb. ●, curve measured as the field is reduced from out-of-plane saturation at 20 kOe; △, curve obtained upon increasing the field from a disordered remanent state. Straight line indicates the linear temperature dependence characteristic of a plain Nb film. Insets are sketches of sample structure.

transition from linear to non-linear $H_{c2}(T)$ behavior, i.e., from extended to confined superconductivity. This results in a lower value of the magnetization at the end of the percolation process and, therefore, in a larger critical percolation threshold $p_c = 0.3$ for copolymer/Nd-Co(52)/Nb than in the rest of the samples that show percolation effects (see Table I). It is interesting to note that, in double percolation systems, an increase in percolation threshold is expected when the scale of one of the percolation levels is reduced,[27] in agreement with a reduction in the size of reverse domain clusters, as domain expansion is hindered by disorder.

IV. CONCLUSIONS

In summary, superconducting and magnetic properties of hybrid Nd-Co/Nb bilayers have been studied at the onset of the magnetization reversal process as a function of magnetic layer thickness and of disorder induced by a nanostructured copolymer template. The comparison between superconducting phase diagrams and out-of-plane hysteresis loops show that a good correspondence between the field range for percolation effects in the superconductor and thee characteristic fields for reverse domain nucleation and fast domain expansion in the magnetic layer extracted from the magnetic hysteresis loops. Low percolation thresholds of the order of 0.2 are found for the disordered superconducting network imprinted by the labyrinth domain, which can be associated to the spatial heterogeneity of domain structure during the stage of fast domain expansion. As disorder increases in the magnetic layer and the magnetization reversal process becomes more homogeneous, the transition from extended to confined superconductivity becomes broader until percolation effects disappear from the superconducting transition of the thinnest copolymer/Nd-Co/Nb sample.

[1]C. Chappert, H. Bernas, J. Ferré, V. Kottler, J. P. Jamet, Y. Chen, E. Cambril, T. Devolder, F. Rousseaux, V. Mathet, and H. Launois, Science **280**, 1919 (1998).
[2]A. Hubert and R. Schafer, *Magnetic Domains* (Springer-Verlag, Berlin, 1998).
[3]A. Schwarz, M. Liebmann, U. Kaiser, R. Wiesendanger, T. W. Noh, and D. W. Kim, Phys. Rev. Lett. **92**, 077206 (2004); A. Hierro-Rodriguez, R. Cid, M. Vélez, G. Rodriguez-Rodriguez, J. I. Martín, L. M. Alvarez-Prado, and J. M. Alameda, Phys. Rev. Lett. **109**, 117202 (2012).
[4]J. E. Davies, O. Hellwig, E. E. Fullerton, G. Denbeaux, J. B. Kortright, and K. Liu, Phys. Rev. B **70**, 224434 (2004).
[5]M. Seul and R. Wolfe, Phys. Rev. A **46**, 7519 (1992).
[6]Z. Yang, M. Lange, A. Volodin, R. Szymczak, and V. V. Moshchalkov, Nature Mater. **3**, 793 (2004).
[7]For a review, see A. I. Buzdin, Rev. Mod. Phys. **77**, 935 (2005).
[8]M. Houzet and A. I. Buzdin, Phys. Rev. **74**, 214507 (2006).
[9]M. Vélez, J. I. Martín, J. E. Villegas, A. Hoffmann, E. M. González, J. L. Vicent, and I. K. Schuller, J. Magn. Magn. Mater. **320**, 2547 (2008) and references therein.
[10]A. Yu Aladyshkin and V. V. Moshchalkov, Phys. Rev. B **74**, 064503 (2006).
[11]L. Y. Zhu, M. Cieplak, and C. L. Chien, Phys. Rev. B **82**, 060503 (2010).
[12]V. Vlasko-Vlasov, U. Welp, G. Karapetrov, V. Novosad, D. Rosenmann, M. Iavarone, A. Belkin, and W. K. Kwok, Phys. Rev. B **77**, 134518 (2008).
[13]L. Ruiz-Valdepeñas, M. Vélez, F. Valdés-Bango, L. M. Alvarez-Prado, J. I. Martín, E. Navarro, J. M. Alameda, and J. L. Vicent, New J. Phys. **15**, 103025 (2013).
[14]F. Valdés-Bango, F. J. García-Alonso, G. Rodríguez-Rodríguez, L. Moran-Fernández, A. Anillo, L. Ruiz-Valdepeñas, E. Navarro, J. L. Vicent, M. Vélez, J. I. Martín, and J. M. Alameda, J. Appl. Phys. **112**, 083914 (2012).
[15]M. S. M. Minhaj, S. Meepagala, J. T. Chen, and L. E. Wenger, Phys. Rev. B **49**, 15235 (1994); Z. Radovic, L. Dobrosavljevic-Grujic, A. I. Buzdin, and J. R. Clem, Phys. Rev. **38**, 2388 (1988).
[16]A. Hierro-Rodríguez, G. Rodríguez-Rodríguez, J. M. Teixeira, G. N. Kakazei, J. B. Sousa, M. Vélez, J. I. Martín, L. M. Alvarez-Prado, and J. M. Alameda, J. Phys. D: Appl. Phys. **46**, 345001 (2013).
[17]J. Diaz, R. Cid, A. Hierro, L. M. Alvarez-Prado, C. Quiros, and J. M. Alameda, J. Phys.: Condens. Matter **25**, 426002 (2013).
[18]A. Lyberatos, J. Earl, and R. W. Chantrel, Phys. Rev. B **53**, 5493 (1996).
[19]L. M. Alvarez-Prado and J. M. Alameda, Physica B **343**, 241 (2004).
[20]M. Cagigal, J. Fontcuberta, M. A. Crusellas, J. L. Vicent, and S. Piñol, Phys. Rev. B **50**, 15993 (1994).
[21]T. R. McGuire and R. J. Potter, IEEE Trans. Magn. **11**, 1018 (1975) and references therein.
[22]A. Yu Aladyshkin, A. I. Buzdin, A. A. Fraerman, A. S. Mel'nikov, D. A. Ryzhov, and A. V. Sokolov, Phys. Rev. B **68**, 184508 (2003).
[23]E. A. Jagla, Phys. Rev. B **72**, 094406 (2005).
[24]A. Benassi and S. Zapperi, Phys. Rev. B **84**, 214441 (2011).
[25]N. Pilet, T. V. Ashworth, M. A. Marioni, H. J. Hug, K. Zhang, and K. P. Lieb, J. Magn. Magn. Mater. **316**, e583 (2007).
[26]Z. Yang, K. Vervaeke, V. V. Moshchalkov, and R. Szymczak, Phys. Rev. B **73**, 224509 (2006).
[27]J. Li, B. Ray, M. A. Alam, and M. Ostling, Phys. Rev. E **85**, 021109 (2012).